Quasi-classical trajectory study of the isotope effect on the stereodynamics in the reaction $H(^2S) + CH(X^2\Pi; v = 0, j = 1) \rightarrow C(^1D) + H_2(X^1\Sigma_g^+)$*

Wang Yun-Hui(王允辉), Xiao Chuan-Yun(肖传云), Deng Kai-Ming(邓开明), and Lu Rui-Feng(陆瑞锋)†

Department of Applied Physics, Nanjing University of Science and Technology, Nanjing 210094, *China*

(Received 11 July 2013; revised manuscript received 26 August 2013; published online 20 February 2014)

The isotope effect on the stereodynamic properties in the title reaction is investigated by a quasi-classical trajectory (QCT) method on the $1^1A'$ potential energy surface at a collision energy of 23.06 kcal/mol. The angular distributions $P(\theta_r)$, $P(\phi_r)$, $P(\theta_r, \phi_r)$, and the polarization-dependent generalized differential cross sections are calculated, which demonstrate the observable influences on the rotational polarization of the product by the isotopic substitution of H with D.

Keywords: quasi-classical trajectory, stereodynamics, isotope effects, product polarization

PACS: 34.50.Lf, 34.50.–s, 31.15.xv, 31.15.ap **DOI:** 10.1088/1674-1056/23/4/043401

1. Introduction

The methylene molecule is an important intermediate in many organic reactions and plays a central role in astrochemical and combustion processes. Especially, the reaction of an electronically excited carbon atom $C(^1D) + H_2$ and its isotopic variants $C(^1D) + HD$ and $C(^1D) + D_2$ have aroused a great interest in the field of physical chemistry. So far, many experimental studies on this system have been done for the angular and the time-of-flight distributions,[1–3] the product internal energy distribution[4–6] as well as the kinetics.[7–9] Being a typical atom–diatom insertion and weak exothermic reaction, it has also been investigated from the theoretical point of view[10–14] by quasi-classical trajectory (QCT)[10,11] and quantum mechanical (QM)[10–14] scattering methods. To our knowledge, for the reverse reactions $H(^2S) + CH(X^2\Pi) \rightarrow C(^3P) + H_2$, and $H(^2S) + CH(X^2\Pi) \rightarrow C(^1D) + H_2$, the former reaction has been studied in theory[15–17] and experiment[18–20] carefully, however, the latter has not been sufficiently studied. Therefore, in this paper, we pay attention to the stereodynamic properties of $H(^2S) + CH(X^2\Pi) \rightarrow C(^1D) + H_2$ and its isotopic variants H + CD, D + CH and D + CD by the QCT approach. In the present study, we employ the BHL potential energy surface (PES)[21] based on the multireference, single and double configuration interaction calculations, which is barrier-less for the perpendicular C_{2v} geometry and has a well depth of 4.33 eV relative to the $C(^1D) + H_2$ asymptote, but presents a large barrier (12.35 kcal/mol) for the collinear $C_{\infty v}$ geometry.

2. Computational details

The QCT method is the same as that in Refs. [22]–[43]. The classical Hamilton equations are numerically integrated in three dimensions. In the center-of-mass (CM) frame shown in Fig. 1, the reagent relative velocity vector $\boldsymbol{k}$ is parallel to the z axis, and the x–z plane is the scattering plane containing the reagent initial vector $\boldsymbol{k}$ and the final product relative velocity vector $\boldsymbol{k}'$, while the y axis is perpendicular to the x–z plane. The scattering angle θ_t represents the angle between the reagent relative velocity and the product relative velocity. The θ_r and ϕ_r are the polar and azimuthal angles of the final rotational angular momentum $\boldsymbol{j}'$.

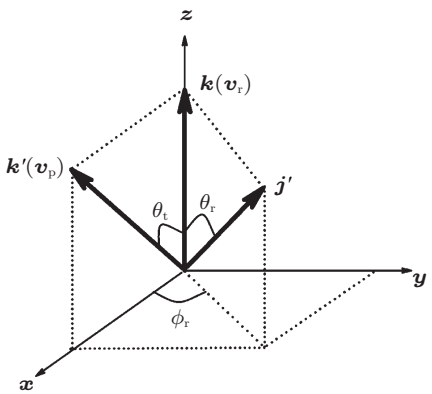


Fig. 1. Center-of-mass frame used to describe the vector properties.

The $\boldsymbol{k}$–$\boldsymbol{j}'$ correlation distribution function $P(\theta_r)$ can be expanded into a series of Legendre polynomials,

$$P(\theta_r) = \frac{1}{2}\sum_k (2k+1) a_0 P_k(\cos\theta_r), \qquad (1)$$

*Project supported by the National Natural Science Foundation of China (Grant No. 11004107) and the Scientific Research Innovation Projects of Jiangsu Province for University Graduate Students, China (Grant No. CXZZ13_0201).

†Corresponding author. E-mail: rflu@njust.edu.cn

© 2014 Chinese Physical Society and IOP Publishing Ltd

$$a_0 = \langle \mathrm{P}_k(\cos\theta_\mathrm{r})\rangle, \tag{2}$$

where the expansion coefficient a_0 is called an orientation or an alignment parameter when the k is odd or even, respectively. The dihedral angular distribution of the $\boldsymbol{k}$–$\boldsymbol{k}'$–$\boldsymbol{j}'$ correlation is characterized by the angle ϕ_r, and the distribution function $P(\phi_\mathrm{r})$ can be presented as a Fourier series,

$$P(\phi_\mathrm{r}) = \frac{1}{2\pi}\left[1 + \sum_{\mathrm{even},n\geq 2} a_n \cos(n\phi_\mathrm{r}) + \sum_{\mathrm{odd},n\geq 1} b_n \sin(n\phi_\mathrm{r})\right], \tag{3}$$

where $a_n = 2\langle\cos(n\phi_\mathrm{r})\rangle$, $b_n = 2\langle\sin(n\phi_\mathrm{r})\rangle$, and n is assumed to meet the requirement of convergence. The joint probability density function $P(\theta_\mathrm{r},\phi_\mathrm{r})$, which is correlated to the direction of the product rotation angular momentum, can be written as

$$P(\theta_\mathrm{r},\phi_\mathrm{r}) = \frac{1}{4\pi}\sum_k \sum_{q\geq 0}\left[a^k_{q\pm}\cos q\phi_\mathrm{r} - a^k_{q\mp}\mathrm{i}\sin q\phi_\mathrm{r}\right] \times \mathrm{C}_{kq}(\theta_\mathrm{r},0), \tag{4}$$

where

$$a^k_{q\pm} = 2\mathrm{i}\langle \mathrm{C}_{kq}(\theta_\mathrm{r},0)\cos(q\phi_\mathrm{r})\rangle, \quad k \text{ is even},$$
$$a^k_{q\pm} = 2\mathrm{i}\langle \mathrm{C}_{kq}(\theta_\mathrm{r},0)\sin(q\phi_\mathrm{r})\rangle, \quad k \text{ is odd},$$

and $\mathrm{C}_{kq}(\theta_\mathrm{r},\theta_t) = \sqrt{4\pi/(2k+1)}Y_{kq}(\theta_\mathrm{r},\theta_t)$.

The fully correlated CM frame angular distribution can be represented by a set of generalized polarization-dependent differential cross sections (PDDCSs) as follows:

$$P(\omega_t,\omega_\mathrm{r}) = \sum_{kq}\frac{[k]}{4\pi}\frac{1}{\sigma}\frac{\mathrm{d}\sigma_{kq}}{\mathrm{d}\omega_t}\mathrm{C}_{kq}(\theta_\mathrm{r},\phi_\mathrm{r})^*, \tag{5}$$

where $[k] = 2k+1$, $\mathrm{d}\sigma_{kq}/(\sigma\,\mathrm{d}\omega_t)$ is a generalized PDDCS and $\mathrm{C}_{kq}(\theta_\mathrm{r},\phi_\mathrm{r})^*$ is the modified conjugate spherical harmonics, and $\mathrm{d}\sigma_{kq}/(\sigma\,\mathrm{d}\omega_t)$ yields

$$\frac{1}{\sigma}\frac{\mathrm{d}\sigma_{k0}}{\mathrm{d}\omega_t} = 0, \quad (k \text{ is odd}), \tag{6}$$

$$\frac{1}{\sigma}\frac{\mathrm{d}\sigma_{kq-}}{\mathrm{d}\omega_t} = \frac{1}{\sigma}\frac{\mathrm{d}\sigma_{kq}}{\mathrm{d}\omega_t} - \frac{1}{\sigma}\frac{\mathrm{d}\sigma_{k-q}}{\mathrm{d}\omega_t} = 0,$$
(k is even, q is even or k is odd, q is odd), (7)

$$\frac{1}{\sigma}\frac{\mathrm{d}\sigma_{kq+}}{\mathrm{d}\omega_t} = \frac{1}{\sigma}\frac{\mathrm{d}\sigma_{kq}}{\mathrm{d}\omega_t} + \frac{1}{\sigma}\frac{\mathrm{d}\sigma_{k-q}}{\mathrm{d}\omega_t} = 0,$$
(k is even, q is odd or k is odd, q is even). (8)

The PDDCS can be calculated by the following formula

$$\frac{1}{\sigma}\frac{\mathrm{d}\sigma_{kq\pm}}{\mathrm{d}\omega_t} = \sum_{k_1}\frac{[k_1]}{4\pi}S^{k_1}_{kq\pm}\mathrm{C}_{k_1-q}(\theta_t,0), \tag{9}$$

where $S^{k_1}_{kq\pm}$ is evaluated using the expected value expression

$$S^{k_1}_{kq\pm} = \langle \mathrm{C}_{k_1 q}(\theta_t,0)\mathrm{C}_{kq}(\theta_\mathrm{r},0)[(-1)^q\mathrm{e}^{\mathrm{i}q\phi_\mathrm{r}} \pm \mathrm{e}^{-\mathrm{i}q\phi_\mathrm{r}}]\rangle. \tag{10}$$

Many photo-initiated bimolecular reaction experiments are sensitive to those polarization moments with $k = 0$ and $k = 2$. In this paper, $(2\pi/\sigma)(\mathrm{d}\sigma_{00}/\mathrm{d}\omega_t)$, $(2\pi/\sigma)(\mathrm{d}\sigma_{20}/\mathrm{d}\omega_t)$, $(2\pi/\sigma)(\mathrm{d}\sigma_{22+}/\mathrm{d}\omega_t)$, and $(2\pi/\sigma)$ $(\mathrm{d}\sigma_{21-}/\mathrm{d}\omega_t)$ are calculated and the nonadiabatic effect is neglected. In the QCT calculation, the PDDCS is expanded up to $k_1 = 7$, which is sufficient for good convergence.

Batches of 10^5 trajectories for each isotopic variant are run on the BHL PES at a collision energy of 23.06 kcal/mol. The collision energy, which is larger than the barrier height (12.35 kcal/mol) for the collinear geometry, is chosen to make the reaction observable. Since the lowest allowed rotational state is $j = 1$ for reactant CH($\mathrm{X}^2\Pi$), we employ its ground vibrational level $v = 0$ and the minimal-allowed rotational state $j = 1$, separately. The impact parameter b_max is computed by calculating 10^5 trajectories at a fixed value of b and systematically increasing b until no reactive trajectories are obtained. Trajectories are started at a distance of 25 Å between H/D and the CM of CH/CD, and the integration step size in the trajectories is chosen to be 0.1 fs, which can guarantee the conservation of the total energy and total angular momentum.

3. Results and discussion

Figure 2(a) shows the variations of angular distribution $P(\theta_\mathrm{r})$ with θ_r for the reaction H + CH and its isotopic variants H + CD, D + CH, D + CD, which represent the $\boldsymbol{k}$–$\boldsymbol{j}'$ correlation of the products HD and D_2. It is clear that the $P(\theta_\mathrm{r})$ distributions peak at $\theta_\mathrm{r} = 90^\circ$ and are symmetric with respect to 90°, which indicates that the product rotational angular momentum vector $\boldsymbol{j}'$ is strongly aligned along the direction perpendicular to the relative velocity. Moreover, the $P(\theta_\mathrm{r})$ distributions are rather broad over all the θ_r range, which demonstrates that the product rotational angular momentum vector $\boldsymbol{j}'$ is almost isotropic along the $\boldsymbol{k}$ direction. However, by comparing the $P(\theta_\mathrm{r})$ distributions among the H + CH and its isotopic variants, we find that the H + CD has the weakest alignment. Under the condition of the same PES, the observed alignment difference should be due to the difference in mass factor (i.e. $\cos^2\beta = m_\mathrm{A}m_\mathrm{C}/(m_\mathrm{A}+m_\mathrm{B})(m_\mathrm{B}+m_\mathrm{C})$ for the reaction A + BC→AB + C),[24,25] and our calculated values of mass factor $\cos^2\beta$ are 0.4613, 0.2857, 0.6148, and 0.4282, for H + CH, H + CD, D + CH, and D + CD, respectively. The alignment difference for the reactant CH and its isotopic CD may originate from the difference in effective barrier induced by the discrepancy between the harmonic zero point energies of the reagents CH and CD. By comparing the reactions D + CH and H + CH, we can see that the alignment of the former is stronger, and similarly, the alignment of the D + CD is stronger than that of H + CD, which are consistent with the explanation based on the mass factor. Furthermore, the product rotational alignment parameter $\langle P_2(\boldsymbol{j}'\cdot\boldsymbol{k})\rangle$ can also reflect the degree of the product rotational polarization, and the cal-

culated values are −0.3452, −0.3482, −0.3614, −0.3722 for H + CH, H + CD, D + CH, D + CD, respectively. There are relatively small differences in the $\langle P_2(\boldsymbol{j}' \cdot \boldsymbol{k})\rangle$ among the reaction systems, and particularly, the reaction D + CD has the strongest product rotational polarization. Besides, we know that the title reactions proceed through a long-lived complex due to the deep well on the 1 ^{1}A′ PES, so it is understandable that when H is substituted by D, the lifetimes of complexes become shorter and the product HD/D_2 keeps a little more information especially about the direction from the reactant.

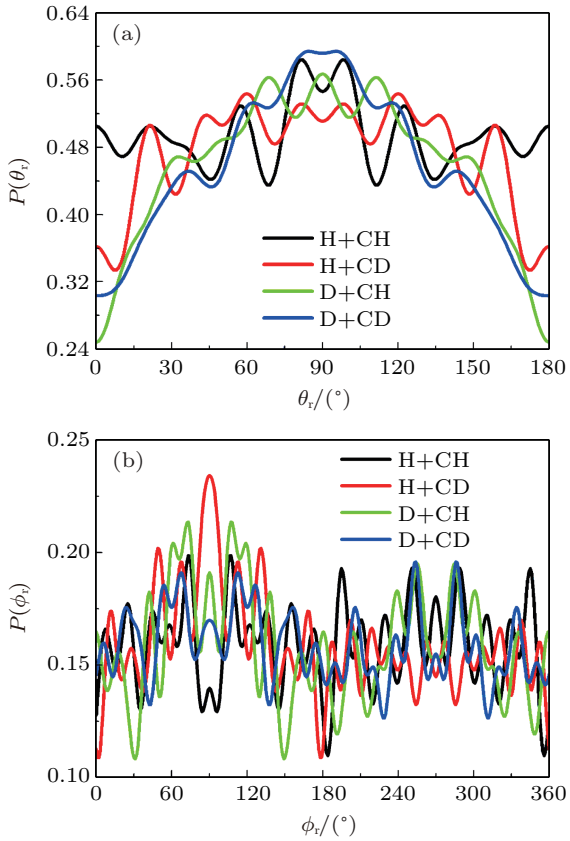


Fig. 2. (color online) (a) Variations of the angular distribution of $P(\theta_r)$ with angle θ_r between $\boldsymbol{k}$ and $\boldsymbol{j}'$ over a range of 0°–180°, and (b) variations of the angular distribution of $P(\phi_r)$ with dihedral angle ϕ_r in a range of 0°–360°.

The variations of dihedral angle distribution $P(\phi_r)$ with ϕ_r are depicted in Fig. 2(b), which reflect the $\boldsymbol{k}$–$\boldsymbol{k}'$–$\boldsymbol{j}'$ correlations of the products. It is shown that the $P(\phi_r)$ distributions are all highly asymmetric with respect to the $\boldsymbol{k}$–$\boldsymbol{k}'$ scattering plane (or at about $\phi_r = 180^\circ$), which indicates the polarizations of the product angular momentum for the four reactions. In addition, there are observable differences in the $P(\phi_r)$ distribution among the four reactions. No obvious single peak can be found in the $P(\phi_r)$ distributions for the H + CH nor for D + CH nor for D + CD reactions. Nevertheless, the $P(\phi_r)$ values for D + CH and D + CD are evidently larger than that for H + CH at the angle close to 90°. That is to say, the orientation of the product rotational angular momentum vector $\boldsymbol{j}'$ along the positive $\boldsymbol{y}$ axis becomes stronger with isotopic substitutions, while the degree of this orientation is generally small. For the H + CH reaction, the $P(\phi_r)$ value at 270° is obviously larger than that at 90°, demonstrating a relatively strong orientation of the product rotational angular momentum vector $\boldsymbol{j}'$ along the negative $\boldsymbol{y}$ axis. In contrast, for the $P(\phi_r)$ distribution of the H + CD reaction, there is a distinct peak at about $\phi_r = 90^\circ$, showing a strong orientation of the product rotational angular momentum vector along the positive $\boldsymbol{y}$ axis.

The reason why the $P(\theta_r)$ distribution is symmetric with respect to $\theta_r = 90^\circ$ while the $P(\phi_r)$ distribution is asymmetric about $\phi_r = 180^\circ$ in these reactions can be interpreted by the impulsive model.[23] According to this model, we have $\boldsymbol{j}' = \boldsymbol{L}\sin^2\beta + \boldsymbol{j}\cos^2\beta + \boldsymbol{J}_1 m_B/m_{AB}$ for the reaction of A + BC → AB + C, where $\boldsymbol{L}$ and $\boldsymbol{j}$ are the reagent orbital and rotational angular momentum, and $\boldsymbol{J}_1 = \sqrt{\mu_{BC}R}(\boldsymbol{r}_{AB} \times \boldsymbol{r}_{BC})$. The μ_{BC} is the reduced mass of the BC molecule, $\boldsymbol{r}_{AB}$ is the unit vector with B pointing to A, $\boldsymbol{r}_{BC}$ is the unit vector of B pointing to C, and R is the repulsive energy between B and C atoms. Starting from the model, when the chemical bond forms and breaks for the title reaction, $\boldsymbol{L}\sin^2\beta + \boldsymbol{j}\cos^2\beta$ is symmetric, while $\boldsymbol{J}_1 m_B/m_{AB}$ shows a preferred direction from the repulsive energy, leading to the asymmetric characteristics of the $P(\phi_r)$ distributions.

In order to validate more information about the angular momentum polarization, we also present the angular distributions in the form of polar plots θ_r and ϕ_r averaged over all scattering angles in Fig. 3. We can see that the $P(\theta_r, \phi_r)$ distribution is symmetric at about $\theta_r = 90^\circ$, while it is asymmetric at about $\phi_r = 180^\circ$. The $P(\theta_r, \phi_r)$ distributions with peaks at (90°, 90°) and (90°, 270°) are in good agreement with the distributions of $P(\theta_r)$ and $P(\phi_r)$ of the corresponding isotopic products, suggesting a favorable polarization of the product perpendicular to the scattering plane.

Figure 4 shows the PDDCSs, which describe the scattering direction of the product molecules H_2, HD, and D_2, as well as the rotational polarization. The PDDCS of $(2\pi/\sigma)(\mathrm{d}\sigma_{00}/\mathrm{d}\omega_t)$ in Fig. 4(a) simply reflects the $\boldsymbol{k}$–$\boldsymbol{k}'$ correlation or the scattering direction of the product, and it is not associated with the alignment and orientation of the product rotational angular momentum vector $\boldsymbol{j}'$. The product molecule prefers forward and backward scatterings that peak at 0° and 180°, albeit the preferences are not significant. The ratios between extreme forward and backward scatterings are 1.16, 1.32, 0.66, and 0.77 for H + CH, H + CD, D + CH, and D + CD reactions, respectively. That is to say, there is a weak forward scattering preference for the H + CH reaction, and the degree of the forward scattering preference is reinforced for H + CD but still weak. As for the reactions D + CH and D + CD, a weak backward scattering can be seen and the degree of the former reaction is stronger than the latter one. The deep well of about 4.3 eV at the exit channel has a great influence on the title reaction, and the scattering preferences of different isotope reactions are sensitive to the reactive activities of the formed long-lifetime complexes (HCH, HCD, and DCD) on the PES.

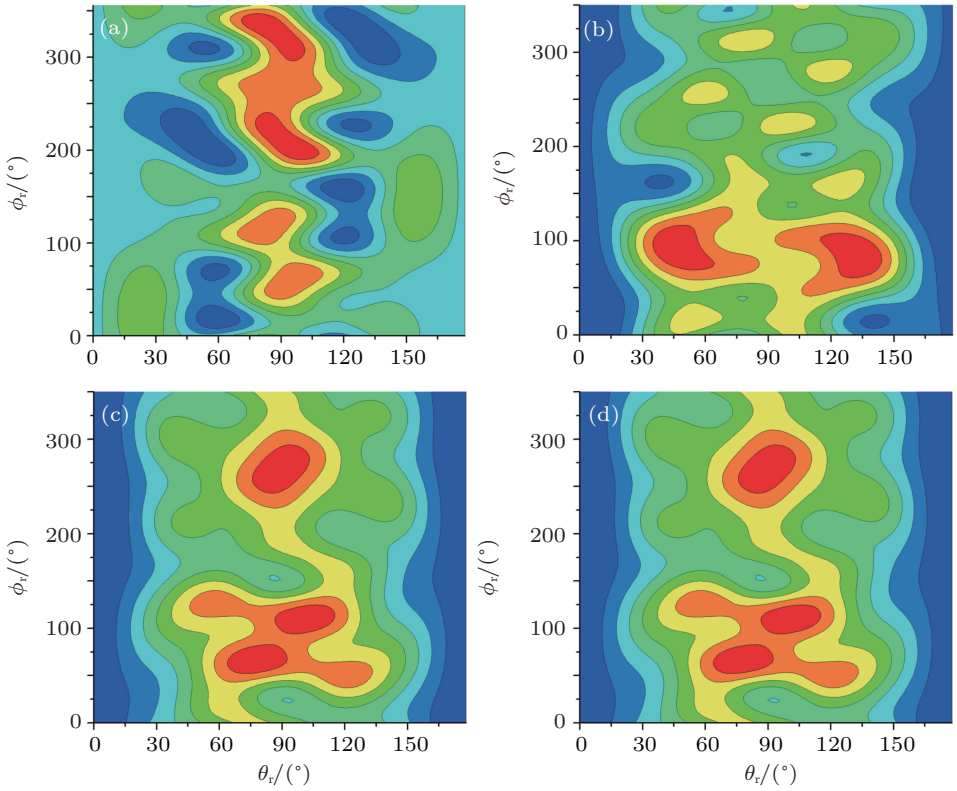


Fig. 3. (color online) Joint probability density distribution of $P(\theta_r, \phi_r)$ as a function of both θ_r and ϕ_r for the reactions of (a) H + CH, (b) H + CD, (c) D + CH, and (d) D + CD.

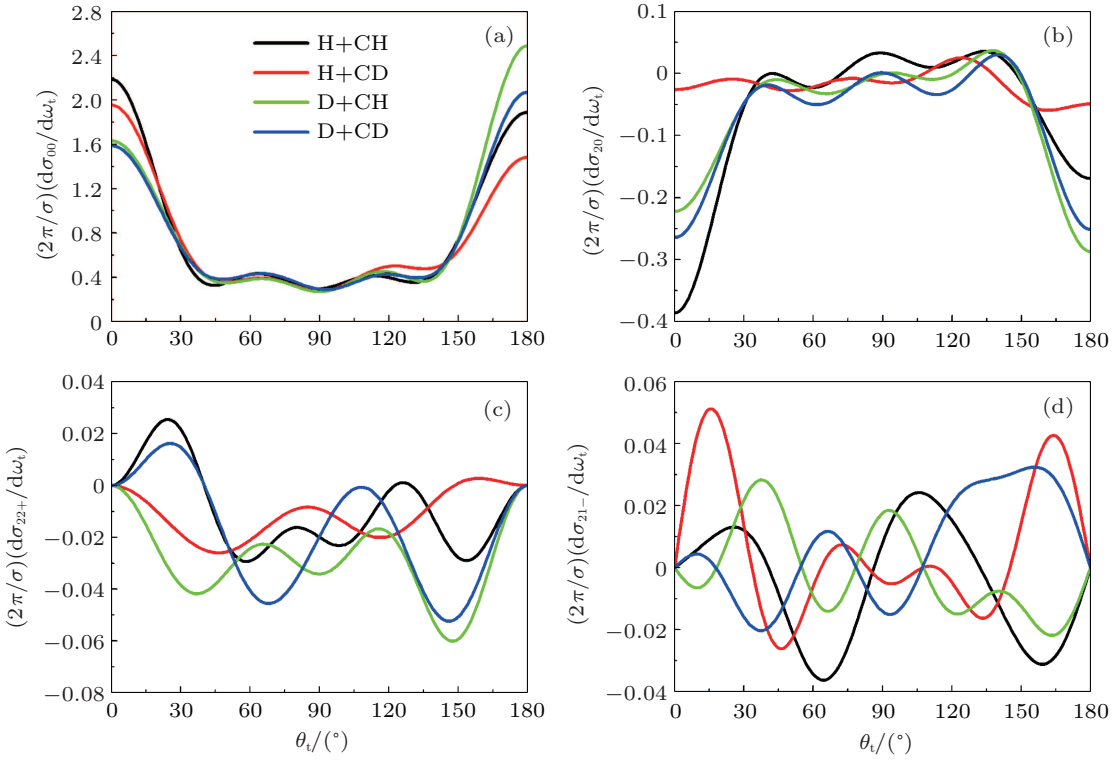


Fig. 4. (color online) The generalized polarization-dependent differential cross sections: (a) $(2\pi/\sigma)(d\sigma_{00}/d\omega_t)$, (b) $(2\pi/\sigma)(d\sigma_{20}/d\omega_t)$, (c) $(2\pi/\sigma)(d\sigma_{22+}/d\omega_t)$, and (d) $(2\pi/\sigma)(d\sigma_{21-}/d\omega_t)$, each as a function of the scattering angle over a range of 0°–180°.

The PDDCS of $(2\pi/\sigma)(d\sigma_{20}/d\omega_t)$ in Fig. 4(b), which is the expectation value of the second Legendre moment $\langle P_2(\cos\theta_r)\rangle$, shows an trend opposite to the behavior of $(2\pi/\sigma)(d\sigma_{00}/d\omega_t)$ in Fig. 4(a) over the range of the scattering angle. This indicates that the product rotational angular momentum $\boldsymbol{j}'$ is aligned in the direction perpendicular to $\boldsymbol{k}$.

From the classical viewpoint, we know that the PDDCS is proportional to $0.5 \times (3\cos^2\theta_r - 1)$, and $(2\pi/\sigma)(d\sigma_{20}/d\omega_t)$ has a classical limiting value of -0.5 at $\theta_r = 90^\circ$. That means that the product rotational angular momentum direction will be most strongly aligned and it is perpendicular to $\boldsymbol{k}$ when $(2\pi/\sigma)(d\sigma_{20}/d\omega_t)$ is equal to -0.5. Therefore, the $\boldsymbol{j}'$ is preferentially polarized along the direction perpendicular to $\boldsymbol{k}$ for the reactions H + CH and D + CD at $\theta_r = 0^\circ$, and for H + CD and D + CH at $\theta_r = 180^\circ$.

The $\boldsymbol{k}$–$\boldsymbol{k}'$ scattering plane is not determined and the value of PDDCS must be zero at the extreme scattering angles when $q \neq 0$. Figure 4(c) shows the calculated $(2\pi/\sigma)(d\sigma_{22+}/d\omega_t)$ distributions, which are correlated to the $\langle \sin^2\theta_r \cos 2\phi_r \rangle$. The values of $(2\pi/\sigma)(d\sigma_{22+}/d\omega_t)$ are positive at $\theta_t = 24^\circ$, $\theta_t = 159^\circ$, and $\theta_t = 26^\circ$ for the reactions H + CH, H + CD, and D + CD, respectively, which indicates that the product alignments are all prone to being primarily along the $\boldsymbol{x}$ axis at these scattering angles. In addition, the values of $(2\pi/\sigma)(d\sigma_{22+}/d\omega_t)$ for the majority are negative, implying that the product alignment tends to be along the $\boldsymbol{y}$ axis. However, there is a noticeable discrepancy in the $(2\pi/\sigma)(d\sigma_{22+}/d\omega_t)$ distribution for the degree of the polarization among the reaction H + CH and its isotopic variants. Furthermore, the negative maximum peaks can be found at two scattering angles around 58° and 154° for the reaction H + CH, demonstrating the strongest polarization at the two scattering angles. Similar situations can be observed, respectively, at the scattering angle of 47° for H + CD, 147° for D + CH and 146° for D + CD, and the product of the reaction D + CH with the strongest alignment tends to be along the $\boldsymbol{y}$ axis. The behaviors of the PDDCSs with $q \neq 0$ at the scattering away from extreme forward and backward directions are more attractive, which provides stereodynamics information about the ϕ_r dihedral angle distribution, and the fact that the values are nonzero at the scattering angles away from $\theta_t = 0^\circ$ and 180° indicates that the $P(\phi_r, \theta_r)$ is not isotropic for sideways and backward scattering products.

The $(2\pi/\sigma)(d\sigma_{21-}/d\omega_t)$ is related to $\langle \cos\theta_r \sin\theta_r \sin\phi_r \rangle$. In Fig. 4(d), we can see clearly that there are large differences among the four isotopic reactions, reflecting the substantial influence on the product polarizations with the isotopic substitution of the H atom. For $(2\pi/\sigma)(d\sigma_{21-}/d\omega_t)$, the positive value indicates the product alignment along the direction of the vector $\boldsymbol{x}$–$\boldsymbol{z}$, and the negative value means the product alignment along the direction of the vector $\boldsymbol{x} + \boldsymbol{z}$. The products have the strongest alignments along the direction of the vector $\boldsymbol{x}$–$\boldsymbol{z}$, respectively, at the scattering angle of 106° for H + CH, 16° for H + CD, 39° for D + CH, and 157° for D + CD. Moreover, the products have the strongest alignments along the direction of the vector $\boldsymbol{x} + \boldsymbol{z}$, respectively, at the scattering angle of 64° for H + CH, 46° for H + CD, 165° for D + CH, and 38° for D + CD.

4. Conclusions

In this paper, we reported on the rotational polarizations of the product for the reaction H + CH and its isotopic reactions on the BHL PES at a collision energy of 23.06 kcal/mol by the QCT method. All the calculated $P(\theta_r)$, $P(\phi_r)$, and $P(\theta_r, \phi_r)$ distributions, as well as four PDDCSs show non-ignorable isotope effects on the alignment and orientation of the product molecules.

Acknowledgment

The authors sincerely thank Prof. Han Ke-Li for providing us with the computational code.

References

[1] Bergeat A, Cartechini L, Balucani N, Capozza G, Philips L F, Casavecchia P, Volpi G G, Bonnet L and Rayez J C 2000 *Chem. Phys. Lett.* **327** 197
[2] Balucani N, Capozza G, Cartechini L, Bergeat A, Bobbenkamp R, Casavecchia P, Aoiz F J, Bañares L, Honvault P, Bussery-Honvault B and Launay J M 2004 *Phys. Chem. Chem. Phys.* **6** 4957
[3] Balucani N, Capozza G, Segoloni E, Bobbenkamp R, Casaveechia P, Gonzalez-Lezana T, Rackham E J, Bañares L and Aoiz J F 2005 *J. Chem. Phys.* **122** 234309
[4] Jursich G M and Wiesenfeld J R 1985 *J. Chem. Phys.* **83** 910
[5] Scott D C, De Juan J, Robie D C, Schwartz-Lavi D and Reisler H 1992 *J. Phys. Chem.* **96** 2509
[6] Mikulecky K and Gericke K H 1993 *J. Chem. Phys.* **98** 1244
[7] Husain D and Norris P E 1979 *Faraday Discuss. Chem. Soc.* **67** 273
[8] Fisher W H, Carrington T, Sadowski C M and Dugan C H 1985 *Chem. Phys.* **97** 433
[9] Sato K, Ishida N, Kurakata T, Iwasaki A and Tsuneyuki S 1998 *Chem. Phys.* **237** 195
[10] Bañares L, Aoiz F J, Honvault P, Bussery-Honvault B and Launay J M 2003 *J. Chem. Phys.* **118** 565
[11] Honvault P, Bussery-Honvault B, Launay J M, Aoiz F J and Bañares L 2006 *J. Chem. Phys.* **124** 154314
[12] Lin S Y and Guo H 2004 *J. Phys. Chem. A* **108** 2141
[13] Defazio P, Gamallo P, González M, Akpinar S, Bussery-Honvault B, Honvault P and Petrongolo C 2010 *J. Chem. Phys.* **132** 104306
[14] Defazio P, Bussery-Honvault B, Honvault P and Petrongolo C 2011 *J. Chem. Phys.* **135** 114308
[15] Harding L B, Guadagnini R and Schatz G C 1993 *J. Phys. Chem.* **97** 5472
[16] van Harrevelt R, van Hemert M C and Schatz G C 2002 *J. Chem. Phys.* **116** 6002
[17] Gamallo P, Defazio P, Akpinar S and Petrongolo C 2012 *J. Phys. Chem. A* **116** 8291
[18] Becker K H, Engelhardt B, Wiesen P and Bayes K D 1989 *Chem. Phys. Lett.* **154** 342
[19] Dean A J, Davidson D F amd Hanson R K 1991 *J. Phys. Chem.* **95** 183
[20] Dean A J and Hanson R K 1992 *Int. J. Chem. Kinet.* **24** 517
[21] Bussery-Honvault B, Honvault P and Launay J M 2001 *J. Chem. Phys.* **115** 10701
[22] Han K L, He G Z and Lou N Q 1996 *J. Chem. Phys.* **105** 8699
[23] Li R J, Han K L, Li F E, Lu R C, He G Z and Lou N Q 1994 *Chem. Phys. Lett.* **220** 281

[24] Wang M L, Han K L and He G Z 1998 *J. Phys. Chem. A* **102** 10204
[25] Wang M L, Han K L and He G Z 1998 *J. Chem. Phys.* **109** 5446
[26] Han K L, Xu D L, He G Z and Lou N Q 2001 *J. Phys. Chem. A* **105** 2956
[27] Zhang W Q and Chen M D 2009 *J. Theor. Comput. Chem.* **8** 1131
[28] Zhang W Q, Cong S L, Zhang C H, Xu X S and Chen M D 2009 *J. Phys. Chem. A* **113** 4192
[29] Zhang W Q, Li Y Z, Xu X S and Chen M D 2010 *Chem. Phys.* **367** 115
[30] Yang T G, Yuan J C, Cheng D H and Chen M D 2013 *Commun. Comput. Chem.* **1** 15
[31] Cheng J, Yue X F and Feng H R 2012 *Chin. Phys. Lett.* **29** 043101
[32] Ma J J 2013 *Acta Phys. Sin.* **62** 023401 (in Chinese)
[33] Xia W Z, Yu Y J and Yang C L 2013 *Acta Phys. Sin.* **62** 023401 (in Chinese)
[34] Li H, Zheng B and Meng Q T 2012 *Acta Phys. Sin.* **61** 153401 (in Chinese)
[35] Li S J, Shi Y, Xie T X and Jin M X 2012 *Chin. Phys. B* **21** 013401
[36] Yu Y J, Xu Q and Xu X W 2011 *Chin. Phys. B* **20** 123402
[37] Zhao J and Luo Y 2011 *Chin. Phys. B* **20** 043402
[38] Zhao J, Xu Y and Meng Q T 2010 *Chin. Phys. B* **19** 063403
[39] Zhang D, Chu T S and Hao C 2013 *Chin. Phys. B* **22** 063401
[40] Zhou S W, Wang Y H and Lu R F 2012 *Chem. Phys.* **402** 113
[41] Lu R F, Wang Y H and Deng K M 2013 *J. Comput. Chem.* **34** 1735
[42] Guo Y H, Zhang F Y and Ma H Z 2013 *Chin. Phys. B* **22** 053402
[43] Guo Y H, Zhang F Y and Ma H Z 2013 *Commun. Comput. Chem.* **1** 99